Applied Catalysis B: Environmental 96 (2010) 361–369

Contents lists available at ScienceDirect

Applied Catalysis B: Environmental

journal homepage: www.elsevier.com/locate/apcatb

Mineralization of the drug β-blocker atenolol by electro-Fenton and photoelectro-Fenton using an air-diffusion cathode for H_2O_2 electrogeneration combined with a carbon-felt cathode for Fe^{2+} regeneration

Eloy Isarain-Chávez, Conchita Arias, Pere Lluís Cabot, Francesc Centellas, Rosa María Rodríguez, José Antonio Garrido, Enric Brillas*

Laboratori d'Electroquímica dels Materials i del Medi Ambient, Departament de Química Física, Facultat de Química, Universitat de Barcelona, Martí i Franquès 1-11, 08028 Barcelona, Spain

ARTICLE INFO

Article history:
Received 19 December 2009
Received in revised form 18 February 2010
Accepted 24 February 2010
Available online 3 March 2010

Keywords:
Pharmaceuticals
Electrochemical advanced oxidation processes
Decay kinetics
Oxidation products
Fe(II) complexes

ABSTRACT

Two-electrode cells with a Pt or boron-doped diamond anode and an air-diffusion cathode for H_2O_2 electrogeneration, and four-electrode combined cells containing the above pair of electrodes coupled in parallel to a Pt anode and a carbon-felt cathode, have been used to degrade the pharmaceutical β-blocker atenolol by electro-Fenton and photoelectro-Fenton methods. In these processes, organics are mainly oxidized with hydroxyl radical (•OH) formed simultaneously at the anode surface from water oxidation and from Fenton's reaction between added catalytic Fe^{2+} and electrogenerated H_2O_2. Aromatic intermediates such as 4-hydroxyphenylacetamide and *p*-benzoquinone and generated carboxylic acids such as maleic, fumaric, tartaric, tartronic, glycolic, formic, oxalic and oxamic are detected and quantified by high-performance liquid chromatography. Compared with the single cells, the corresponding novel four-electrode combined systems enhance strongly the mineralization rate of atenolol in electro-Fenton because of the fast Fe^{2+} regeneration at the carbon-felt cathode favoring: (i) the production of more amounts of •OH from Fenton's reaction that destroy more rapidly aromatic pollutants and (ii) the formation of Fe(II) complexes with final carboxylic acids such as oxalic and oxamic, which are more quickly oxidized with •OH. In photoelectro-Fenton, both single and combined cells show a quite similar oxidation power giving almost total mineralization as a result of the parallel quick photolysis of Fe(III) and/or Fe(II) complexes under UVA irradiation. The efficient regeneration of Fe^{2+} with larger •OH production in the combined cells causes a quicker atenolol decay, which always follows a pseudo first-order reaction. NH_4^+ and in smaller proportion NO_3^- are always released to the medium.

1. Introduction

There is an increasing interest in the study of the destruction of persistent organic pollutants (POPs) in wastewaters by advanced oxidation processes (AOPs), which are environmentally friendly chemical, photochemical, photocatalytic and electrochemical methods based on the in situ generation of hydroxyl radical (•OH) [1–3]. This radical is the second strongest oxidant known after fluorine, with so high standard reduction potential (E°(•OH/H_2O) = 2.80 V/SHE) that non-selectively reacts with POPs until their total mineralization, i.e., overall conversion into CO_2, water and inorganic ions.

Electrochemical advanced oxidation processes (EAOPs) involving indirect electro-oxidation methods with H_2O_2 electrogeneration have received great attention for water remediation since they are simple, inexpensive and allow achieving a large mineralization degree of contaminants. In such procedures, H_2O_2 is continuously supplied to the contaminated solution from the two-electron reduction of O_2 from reaction (1), usually taking place at carbon-felt (CF) [3–10], O_2-diffusion [5,6,11–21] and graphite [3,13] cathodes:

$$O_{2(g)} + 2H^+ + 2e^- \rightarrow H_2O_2 \quad (1)$$

Among these cathodes, it has been found that gas-diffusion electrodes fed with air or oxygen allow the greatest H_2O_2 production in acid medium [3,5,6,13,16].

The most popular EAOP is electro-Fenton (EF) where the oxidizing power of electrogenerated H_2O_2 is strongly enhanced by adding a small quantity of Fe^{2+} as catalyst to the acidic solution, usually at the optimum pH of ca. 3.0, generating the strong oxidant •OH along

* Corresponding author. Tel.: +34 93 4021223; fax: +34 93 4021231.
E-mail address: brillas@ub.edu (E. Brillas).

0926-3373/$ – see front matter © 2010 Elsevier B.V. All rights reserved.
doi:10.1016/j.apcatb.2010.02.033

with Fe^{3+} from Fenton's reaction (2) [22]:

$$Fe^{2+} + H_2O_2 \rightarrow Fe^{3+} + {}^{\bullet}OH + OH^- \quad (2)$$

Reaction (2) is catalytic and can be propagated from Fe^{2+} regeneration that mainly takes place by reduction of Fe^{3+} at the cathode via reaction (3) [4–6], thereby competing with reaction (1):

$$Fe^{3+} + e^- \rightarrow Fe^{2+} \quad (3)$$

The rate of reaction (3) depends on the cathode nature and its ability on H_2O_2 electrogeneration. For a CF electrode with a large 3D active surface and low H_2O_2 production, this reaction is so fast that a large proportion of Fe^{2+} remains in the O_2-saturated contaminated solution. In contrast, for an O_2-diffusion electrode where reaction (1) is preponderant giving rise to a very high H_2O_2 production, reaction (3) is very slow and most iron species are in the form of Fe^{3+} [5,6]. As a result, EF with a CF cathode can yield almost overall mineralization of POPs, even working with divided cells, because Fe(II) complexes formed in large extent can be oxidized with $^{\bullet}OH$ [5,7]. For EF with an O_2-diffusion cathode, however, poorer decontamination is achieved because complexes of Fe(III) with generated carboxylic acids cannot be destroyed by the above radical [11,12]. In this case, the degradation rate can be enhanced using undivided cells with a high O_2 overvoltage anode (M) able to generate heterogeneous hydroxyl radical (M($^{\bullet}OH$)) as intermediate from water oxidation to O_2 at its surface via reaction (4) [2,3]:

$$M + H_2O \rightarrow M({}^{\bullet}OH) + H^+ + e^- \quad (4)$$

Boron-doped diamond (BDD) thin film or Pt has been employed as anodes in EF [18,19,21]. Since the former material possesses much greater O_2 overvoltage, higher amounts of reactive BDD($^{\bullet}OH$) than Pt($^{\bullet}OH$) are produced from reaction (4) under comparable conditions yielding faster degradation of POPs [2]. The destruction of organics in these EF systems is then very complex, taking place via reaction in parallel with homogeneous $^{\bullet}OH$ and heterogeneous BDD($^{\bullet}OH$) or Pt($^{\bullet}OH$).

Another way to accelerate the degradation process is the application of the photoelectro-Fenton (PEF) method [3,11,12,14,15,18,19,21]. In this EAOP, the solution treated under EF conditions is exposed to UVA irradiation, which can produce: (i) greater $^{\bullet}OH$ generation and Fe^{2+} regeneration by photolysis of $Fe(OH)^{2+}$, the predominant Fe^{3+} species at pH 3.0, by reaction (5) [22,23] and (ii) the photolysis of complexes of Fe(III) with generated carboxylic acids. This is the case of Fe(III)-oxalate complexes ($Fe(C_2O_4)^+$, $Fe(C_2O_4)_2^-$ and $Fe(C_2O_4)_3^{3-}$) that undergo fast photodecarboxylation by reaction (6) [24], producing Fe^{2+} regeneration and acceleration of the mineralization process.

$$Fe(OH)^{2+} + h\nu \rightarrow Fe^{2+} + {}^{\bullet}OH \quad (5)$$

$$2Fe(C_2O_4)_n^{(3-2n)} + h\nu \rightarrow 2Fe^{2+} + (2n-1)C_2O_4{}^{2-} + 2CO_2 \quad (6)$$

In previous work, we have tested the EF and/or PEF decontaminations of wastewaters containing some common pharmaceuticals including antimicrobials, analgesics, biocides and non-steroidal anti-inflammatory drugs (NSAIDs) [5,6,14,15,18,19,21]. These EAOPs have been applied using undivided single cells of 100 ml with a BDD or Pt anode and a carbon-polytetrafluoroethylene (PTFE) O_2-diffusion cathode with the aim of developing powerful oxidation methods for the removal of drugs from wastewaters. Because of the widespread consume of pharmaceuticals in human and veterinary medicine, and agricultural and consumer products, along with their inefficient destruction in sewage treatment plants (SWTs), a large variety of these compounds at low contents of micrograms per liter have been detected in surface, ground and drinking waters [25–31]. These contaminants have to be removed from the aquatic environment because can develop multi-resistant strains of microorganisms, can affect the endocrine system of fishes and can exert toxic effects on algae and invertebrates [28,31].

To try obtaining a faster degradation of drugs by the above EAOPs, we have explored a novel cell configuration involving the combination of two cells in parallel, one with a BDD or Pt anode and an air-diffusion electrode (ADE) as cathode and the other one with a Pt anode and a CF cathode. In this coupling, it is expected that the former cell ensures the H_2O_2 electrogeneration from reaction (1) and the oxidative action of BDD($^{\bullet}OH$) or Pt($^{\bullet}OH$) formed from reaction (4) on pollutants, whereas the latter cell operates at much lower current to largely regenerate Fe^{2+} from Fe^{3+} reduction at the CF cathode from reaction (3), producing more quantity of $^{\bullet}OH$ via Fenton's reaction (2). The oxidation ability of these cells has been proven for atenolol (4-(2-hydroxy-3-isopropylaminopropoxy)phenylacetamide), which was chosen as a model molecule of pharmaceutical β-blockers. This drug is widely used for the treatment of angina, glaucoma and high blood pressure, although it is not appreciably metabolized in humans being excreted and accumulated in the environment, where it has been detected up to 10 $\mu g\,l^{-1}$ in SWT effluent discharges [29–31] and surface waters [26,27]. Several studies have revealed its toxicity on algae [25] and freshwater fish species [31]. However, only few papers have recently reported some attempts to oxidize atenolol from diperiodatocuprate(III) in aqueous alkaline medium [32] and from a biological Fenton-like system mediated by the white-rot fungus *Trametes versicolor* [33].

This paper presents a study on the EF and PEF degradations of atenolol using single and the novel combined cells with BDD and/or Pt anodes and ADE and/or CF cathodes. Drug contents much higher than those found in the environment were tested to more clearly ascertain the different action of generated hydroxyl radicals ($^{\bullet}OH$, BDD($^{\bullet}OH$) and/or Pt($^{\bullet}OH$)) and UVA irradiation for explaining the comparative degradation rate of the above EAOPs, the influence of experimental variables and the decay kinetics of the drug. Aromatic intermediates, generated carboxylic acids and released inorganic ions were detected and quantified by several chromatographic techniques. Based on these by-products, a reaction sequence for atenolol mineralization is proposed.

2. Experimental

2.1. Chemicals

Atenolol of 99% purity was supplied by the pharmaceutical AstraZeneca España (Madrid, Spain). 4-Hydroxyphenylacetamide and *p*-benzoquinone were analytical reagent from Aldrich. Tartaric, maleic, fumaric, tartronic, glycolic, oxamic, oxalic and formic acids were reagent or analytical grade from Panreac and Avocado. Sulfuric acid, anhydrous sodium sulfate, ferrous sulfate heptahydrate and ferric sulfate pentahydrate were analytical grade from Merck and Fluka. All solutions were prepared with pure water obtained from a Millipore Milli-Q system with resistivity >18 MΩ cm at 25 °C. Organic solvents and other chemicals used were either HPLC or analytical grade purchased from Merck, Fluka and Aldrich.

2.2. Apparatus

The solution pH was measured with a Crison GLP 22 pH-meter. The power sources used for the electrochemical trials at constant currents were an Amel 2053 potentiostat–galvanostat and/or an EG&G P.A.R. 363 potentiostat–galvanostat. Colorimetric measurements were made with a Unicam UV4 UV/vis Prisma double-beam spectrophotometer thermostated at 25 °C. Total organic carbon (TOC) of solutions was obtained with a Shimadzu VCSN TOC analyzer. Aromatic intermediates were identified by

GC–MS using a Hewlett-Packard system composed of a HP 5890 Series II gas chromatograph fitted with a non-polar J&W DB-5MS 0.25 μm, 30 m × 0.25 mm, column and a HP 5989A mass spectrophotometer in electron impact mode at 70 eV. The temperature ramp was 50 °C for 3 min, 10 °C min^{-1} up to 300 °C and hold time 5 min, while the temperature of the inlet, transfer line and detector was 250, 290 and 300 °C, respectively. The atenolol decay and the evolution of aromatic intermediates were followed by reversed-phase HPLC with a Waters system consisting of a Waters 600 high-performance liquid chromatograph fitted with a Spherisorb ODS2 5 μm, 150 mm × 4.6 mm, column at 35 °C, and coupled with a Waters 996 photodiode array detector selected at λ = 225 nm for atenolol, λ = 224 nm for 4-hydroxyphenylacetamide and λ = 245 nm for *p*-benzoquinone. Carboxylic acids were detected by ion-exclusion chromatography, using the above liquid chromatograph fitted with a Bio-Rad Aminex HPX 87H, 300 mm × 7.8 mm, column at 35 °C and the photodiode array detector selected at λ = 210 nm. Ionic chromatography was made with a Shimadzu 10 Avp HPLC coupled with a Shimadzu CDD 10 Avp conductivity detector, using a Shodex IC YK-421, 125 mm × 4.6 mm, cation column at 40 °C to determine NH_4^+ and a Shim-Pack IC-A1S, 100 mm × 4.6 mm, anion column at 40 °C to obtain NO_3^-.

2.3. Electrolytic systems

A scheme of the experimental set-up used for atenolol treatment by EF and PEF methods in the novel four-electrode combined cells is presented in Fig. 1. All electrolyses were conducted in an open and undivided tank reactor containing 100 ml of solution stirred with a magnetic bar at 800 rpm. Its temperature was regulated at 35 °C by circulating external thermostated water through the double-jacket of the cell. The anodes were a Pt sheet of 99.99% purity from SEMPSA (Barcelona, Spain) or a BDD thin film from Adamant Technologies (La Chaux-de-Fonds, Switzerland). The cathodes were a CF from Sofacel (Sant Feliu, Spain) or a carbon-PTFE ADE from E-TEK (Somerset, NJ, USA). The preparation of the latter cathode has been described [11] and it was fed with an air flow rate of 20 ml min^{-1} to continuously electrogenerate H_2O_2 from reaction (1). The geometric area of all electrodes in contact with the solution was 3 cm^2. Four configurations with monopolar connection, two of them with a pair of electrodes and the other ones with alternated four electrodes, were utilized: (i) Pt/ADE, (ii) BDD/ADE, (iii) combined Pt/ADE-Pt/CF and (iv) combined BDD/ADE-Pt/CF. An independent constant current was then applied to each pair of electrodes, using one or two power sources for single or combined cells, respectively. Atenolol degradation was studied in acidic aqueous media with 0.05 M Na_2SO_4 and H_2SO_4 for pH regulation, with a catalytic concentration of $FeSO_4$. In PEF, the solution was irradiated with a Philips TL/6W/08 fluorescent black light blue tube of λ_{max} = 360 nm, placed at the top of the open cell at 2 cm above the solution and giving a photoionization energy input of 1.4 W m^{-2}, as detected with a NRC 820 laser power meter.

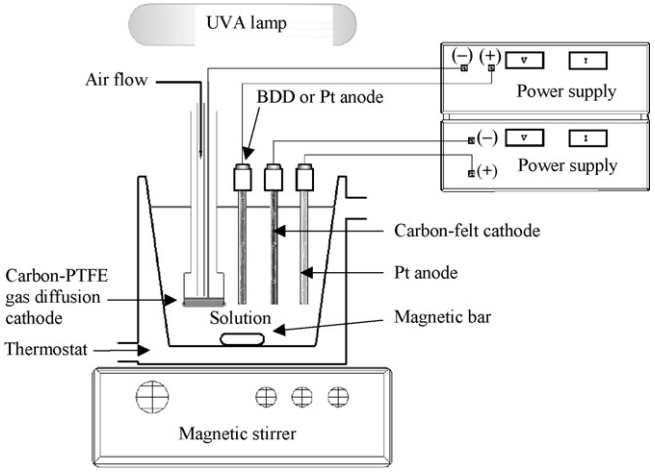

Fig. 1. Sketch of the experimental set-up used for the degradation of 100 ml of atenolol solutions by electro-Fenton (EF) and photoelectro-Fenton (PEF) processes using a four-electrode combined cell with monopolar connection. The anodes were a boron-doped diamond (BDD) thin film and/or Pt sheet, while the cathodes were a carbon-felt (CF) and/or carbon-PTFE air-diffusion electrode (ADE). The geometrical area of all electrodes in contact with the solution was 3 cm^2. A 6-W UVA light (λ_{max} = 360 nm) was utilized in PEF.

2.4. Product analysis procedures

Before analysis, samples withdrawn from treated solutions were filtered with 0.45 μm PTFE filters from Whatman. The concentration of accumulated H_2O_2 was determined from the light absorption of its Ti(IV) colored complex at λ = 409 nm [34]. Fe^{2+} and Fe^{3+} contents were obtained from the light absorption of their corresponding colored complexes with 1,10-phenantroline at λ = 508 nm [35] and with SCN^- at λ = 466 nm [36]. TOC values with an accuracy of ±1% were determined by injecting 50 μl aliquots to the TOC analyzer. For HPLC measurements, 20 μl aliquots were injected to the chromatograph and the mobile phase was a 30:70 (v/v) methanol/phosphate buffer (pH 3.0) mixture, with 1.1 g of sodium heptanesulfonate and 2 ml of di-*n*-butylamine per liter, at 0.6 ml min^{-1} for reversed-phase HPLC and a 4 mM H_2SO_4 solution at 0.6 ml min^{-1} for ion-exclusion HPLC. Ionic chromatography was performed with 25 μl aliquots using aqueous mobile phases of 5.0 mM tartaric acid, 2.0 mM dipicolinic acid, 24.2 mM boric acid and 15.0 mM corona ether at 1.0 ml min^{-1} for NH_4^+ and of 1.0 mM *p*-hydroxybenzoic acid and 1.1 mM *N*,*N*-diethylethanolamine at 1.5 ml min^{-1} for NO_3^-.

To identify the aromatic intermediates formed during atenolol degradation by GC–MS, 15 ml of short-time electrolyzed solutions by EF in a Pt/ADE cell were lyophilized. The remaining products were dissolved in: (i) 2 ml of ethyl acetate or (ii) 2 ml ethanol to obtain the corresponding ethylated derivatives after filtration and addition of 0.05 ml of concentrated HCl under stirring and heating at 60 °C for 15 min.

3. Results and discussion

3.1. Catalytic behavior of the cells

The ability of single and combined cells for H_2O_2 electrogeneration and Fe^{2+} regeneration was checked using a 0.05 M Na_2SO_4 solution with 0.5 mM iron ions at pH 3.0. For a Pt/CF cell without O_2 bubbling through the medium, the same steady Fe^{2+} and Fe^{3+} contents were achieved starting from a 0.5 mM Fe^{2+} or 0.5 mM Fe^{3+} solution without H_2O_2 production. For example, Fig. 2a shows that steady-states with 0.44 mM Fe^{2+} and 0.06 mM Fe^{3+} are obtained after 30 min of electrolysis at 12 mA. Note that similar behavior was found operating from 4 to 12 mA, but the use of greater currents gradually promoted higher Fe^{3+} contents in detriment of Fe^{2+}. At 30 mA, for example, steady concentrations of 0.38 mM for Fe^{2+} and 0.12 mM for Fe^{3+} were determined. This trend can be explained by the predominance of Fe^{2+} regeneration at the CF cathode from reaction (3) over its oxidation at the Pt anode by reaction (7) up to 12 mA, whereas higher currents cause a greater acceleration of the latter reaction respect to the former producing a larger proportion of steady Fe^{3+}. An optimized current of 12 mA was then applied to the Pt/CF cell when used in combined configurations in further

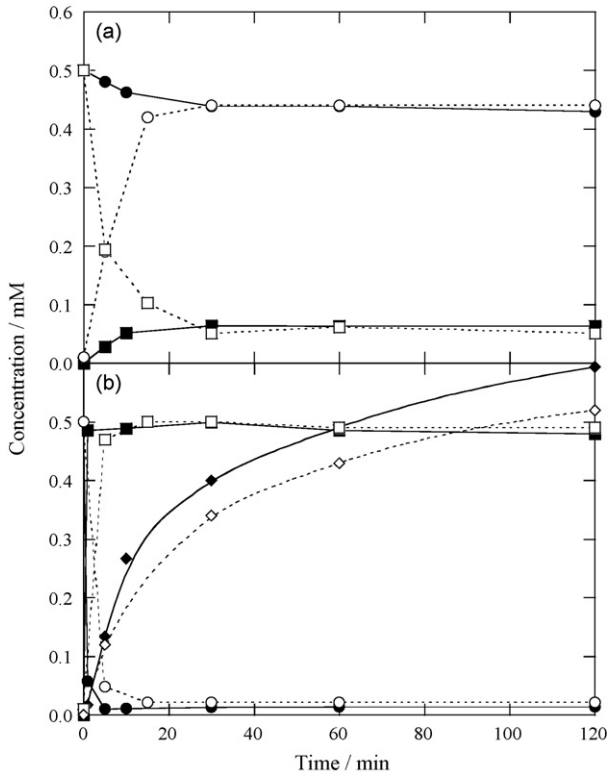

Fig. 2. Time-course evolution of the concentration of (○, ●) Fe^{2+}, (□, ■) Fe^{3+} and (◊, ♦) accumulated H_2O_2 during the electrolysis of 100 ml solutions containing 0.05 M Na_2SO_4 at pH 3.0 and 35 °C. (a) Pt/CF cell at 12 mA starting from 0.5 mM Fe^{2+} (filled symbols) or 0.5 mM Fe^{3+} (empty symbols). (b) The solution contained 0.5 mM Fe^{2+} and it was electrolyzed either in a BDD/ADE cell at 50 mA (filled symbols) or in a combined BDD/ADE–Pt/CF cell at 50–12 mA (empty symbols).

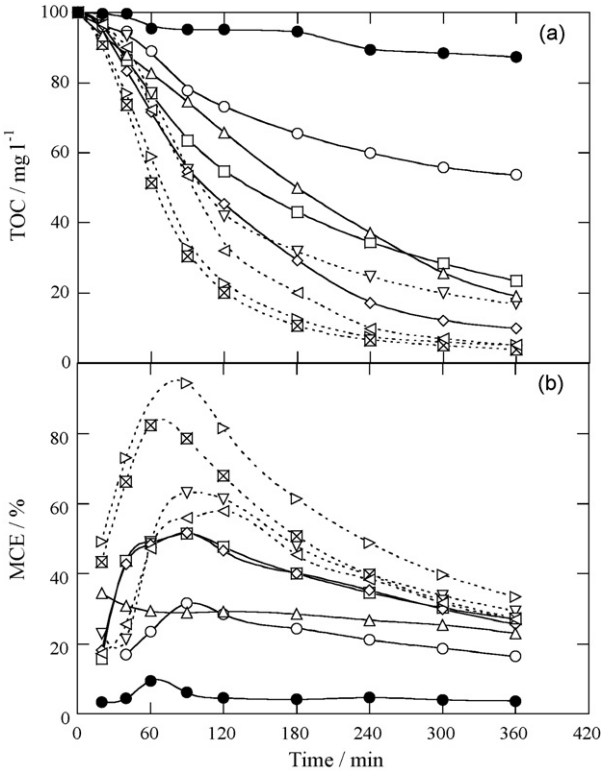

Fig. 3. (a) TOC removal and (b) mineralization current efficiency with electrolysis time for the degradation of 100 ml of a 158 mg l^{-1} atenolol solution in 0.05 M Na_2SO_4 with 0.5 mM Fe^{2+} at pH 3.0 and 35 °C. Method: (●) Oxidation in Pt/CF cell at 12 mA, (○) EF in Pt/ADE cell at 50 mA, (□) EF in BDD/ADE cell at 50 mA, (△) EF in combined Pt/ADE–Pt/CF cell at 50–12 mA, (◊) EF in combined BDD/ADE–Pt/CF cell at 50–12 mA, (▽) PEF in Pt/ADE cell at 50 mA, (▷) PEF in BDD/ADE cell at 50 mA, (◁) PEF in combined Pt/ADE–Pt/CF cell at 50–12 mA and (⊠) PEF in combined BDD/ADE–Pt/CF cell at 50–12 mA.

experiments.

$$Fe^{2+} \rightarrow Fe^{3+} + e^- \quad (7)$$

In the BDD/ADE cell, a rapid oxidation of Fe^{2+} to Fe^{3+} with electrogenerated H_2O_2 via Fenton's reaction (2) occurs, although a low steady content is reached as a result of its regeneration at the cathode by reaction (3). Fig. 2b evidences that operating at 50 mA, steady 0.013 mM Fe^{2+} and 0.48 mM Fe^{3+} are obtained in such a cell after 10 min of electrolysis. Nevertheless, H_2O_2 is progressively accumulated up to ca. 0.6 mM in 120 min since it is efficiently produced at the cathode by reaction (1) and more slowly consumed by Fenton's reaction (2) and its direct oxidation to O_2 at the BDD anode [11]. Fig. 2b also shows a similar evolution for both iron ions in a combined BDD/ADE–Pt/CF cell by independently applying 50 and 12 mA (denoted as 50–12 mA) at the corresponding pair of electrodes. For this system, however, the steady Fe^{2+} content is 0.021 mM, significantly higher than 0.013 mM found for a BDD/ADE cell, as expected if it is quickly regenerated at the CF cathode. This faster Fe^{2+} regeneration also justifies the smaller H_2O_2 accumulation of about 0.5 mM determined after 120 min of electrolysis in the combined cell, as shown in Fig. 2b. In subsection below, this behavior will allow to explain the enhancement of atenolol degradation by EAOPs using such kind of combined cells.

3.2. Comparative TOC removal in single and combined cells

The EF and PEF treatments of 100 ml of a 158 mg l^{-1} atenolol solution (corresponding to 100 mg l^{-1} TOC) with 0.5 mM Fe^{2+} of pH 3.0 were comparatively tested by the different systems to clarify their relative oxidation power. A current of 50 mA was chosen for all Pt/ADE and BDD/ADE cells and the optimized 12 mA for the Pt/CF cell. A progressive mineralization of the drug solution with prolonging electrolysis time to 360 min was found in all cases, while the solution pH decayed up to 2.7–2.8 as maximum owing to the production of acidic by-products.

Fig. 3a depicts that the direct use of the Pt/CF system (without H_2O_2 production) only leads to 13% decontamination at the end of electrolysis, indicating the low ability of Pt(•OH) formed from reaction (4) to mineralize the organic pollutants. In contrast, a much higher degradation rate can be observed for all EF treatments, as expected by the quicker destruction of atenolol and its by-products with •OH generated from Fenton's reaction (2) between electrogenerated H_2O_2 and added Fe^{2+}. Thus, TOC is reduced by 46 and 77% for the Pt/ADE and BDD/ADE single cells, respectively, in 360 min. The higher oxidation power of the latter cell can be related to the greater oxidative ability of reactive BDD(•OH) than Pt(•OH) [2]. These mineralization degrees rise strongly to 81 and 90% for the corresponding combined Pt/ADE-Pt/CF and BDD/ADE-Pt/CF configurations. This behavior corroborates the fast Fe^{2+} regeneration at the CF cathode, enhancing the rate of Fenton's reaction (2) to produce more quantity of •OH that accelerates the removal of organics in both systems.

Fig. 3a also shows a much quicker atenolol degradation for the PEF processes, with raising oxidation power in the sequence Pt/ADE < Pt/ADE-Pt/CF < BDD/ADE ≤ BDD/ADE-Pt/CF. Almost total mineralization (≥95% TOC removal) is achieved in 360 min for the three latter systems. Compared with the EF treatments, the fastest decontamination in analogous PEF processes can be related to the increase in Fe^{2+} regeneration from the photolytic reaction (5), along

with the photodecomposition of Fe(II) and Fe(III) complexes with intermediates.

The above results demonstrate that the combination of two pairs of electrodes with an ADE cathode for H_2O_2 electrogeneration and a CF cathode for Fe^{2+} regeneration enhances the EF and PEF degradations of atenolol. The use of combined cells is very notable for EF where •OH formed from Fenton's reaction (2) plays the most important oxidative role and hence, the increase in Fe^{2+} regeneration strongly accelerates the mineralization process. In PEF, however, the potent synergistic action of UVA irradiation to rapidly degrade organics makes less significant the effect of combining both cathodes (see Fig. 3a). This behavior can be better analyzed by calculating the mineralization current efficiency (MCE, in %) for the above trials at a given time t (h) from Eq. (8) [21]:

$$\mathrm{MCE} = \frac{nFV_s\Delta(\mathrm{TOC})_{\mathrm{exp}}}{4.32\times10^7 mIt} \quad (8)$$

where F is the Faraday constant (96,487 C mol^{-1}), V_s is the solution volume (l), $\Delta(\mathrm{TOC})_{\mathrm{exp}}$ is the experimental TOC decay (mg l^{-1}), 4.32×10^7 is a conversion factor to homogenize units (3600 s h^{-1} × 12,000 mg mol^{-1}), m is the number of carbon atoms of atenolol (14 C atoms) and I is the applied total current (A). The number n of electrons consumed per atenolol molecule during mineralization was taken as 66 considering that it is converted into carbon dioxide and ammonium ion (see below) following reaction (9):

$$C_{14}H_{22}N_2O_3 + 25H_2O \rightarrow 14CO_2 + 2NH_4^+ + 64H^+ + 66e^- \quad (9)$$

Efficiencies thus determined for the experiments of Fig. 3a are presented in Fig. 3b. A maximum MCE value can be usually observed at 60–90 min of all treatments, indicating a fast conversion of several by-products into CO_2 at the early stages of the processes followed by a deceleration at long electrolysis times as a consequence of the loss of organic matter and the formation of more difficultly oxidizable species such as carboxylic acids. Despite the faster degradation rate of atenolol using the combined cells for both EF and PEF methods, results of Fig. 3b show changes in the efficiency trend because the total current of 62 mA applied to these systems is higher than 50 mA of the analogous single cells. Thus, in EF only the MCE values for the Pt/ADE–Pt/CF cell are superior to those of the Pt/ADE one, being higher, but very similar, for the BDD/ADE and BDD/ADE–Pt/CF systems. For the Pt/ADE–Pt/CF cell, however, the efficiency remains practically constant with electrolysis time. This anomalous trend can be related to the fast Fe^{2+} regeneration on the CF cathode that produces much larger amounts of •OH from Fenton's reaction (2) than of Pt(•OH) at the anode, giving rise to a similar destruction rate of all organics during electrolysis. As expected, the analogous PEF treatments yield much greater efficiencies, increasing in the sequence Pt/ADE–Pt/CF ≤ Pt/ADE < BDD/ADE–Pt/CF ≤ BDD/ADE. For the more potent and efficient two latter systems, maximum MCE values as high as 83 and 94% are obtained, respectively, at ca. 60 min. These findings confirm that the above combined cells are clearly preferable to be used in EF, whereas in PEF they are not so useful since they lead to faster degradation but with lower efficiency.

3.3. Effect of experimental variables

The influence of applied current, pH and initial drug concentration on the oxidation power of combined cells was also examined. Fig. 4 exemplifies typical results obtained for the most potent PEF process using a BDD/ADE–Pt/CF cell. Similar behavior was found for the other combined systems tested. As can be seen in Fig. 4a, an increase in current from 25 to 100 mA for the BDD/ADE system, maintaining 12 mA for the Pt/CF one, causes a quicker TOC decay for

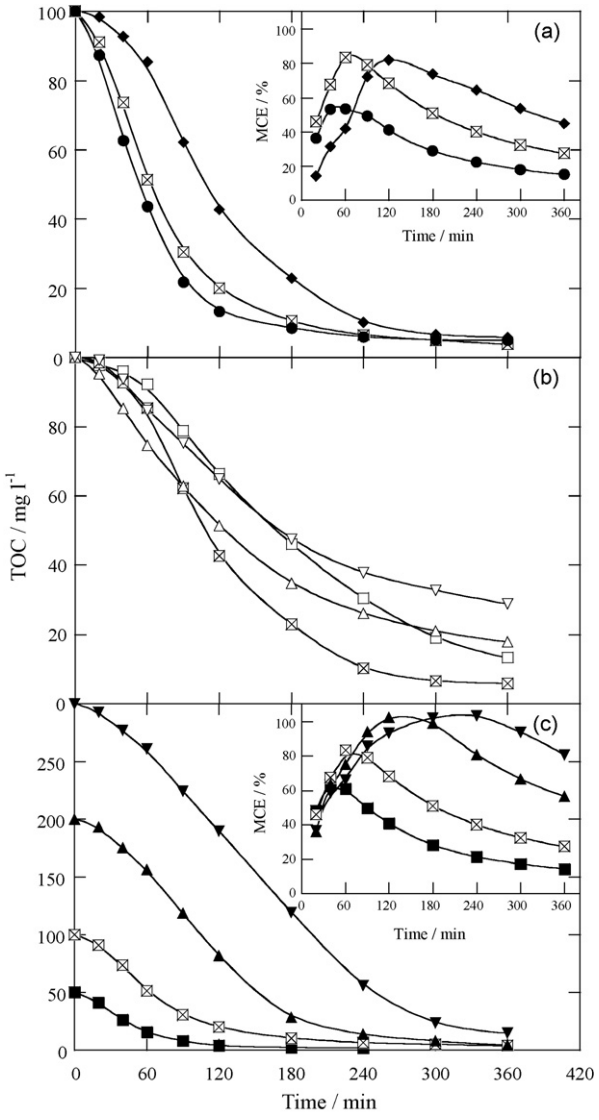

Fig. 4. Influence of experimental parameters on TOC abatement of 100 ml of atenolol solutions in 0.05 M Na_2SO_4 with 0.5 mM Fe^{2+} at 35 °C using PEF in a combined BDD/ADE–Pt/CF cell. (a) 158 mg l^{-1} of atenolol at pH 3.0 by applying: (♦) 25–12, (⊠) 50–12 and (●) 100–12 mA. (b) 158 mg l^{-1} of atenolol at pH: (□) 2.0, (⊠) 3.0, (△) 4.0 and (▽) 6.0 electrolyzed at 50–12 mA. (c) (■) 79, (⊠) 158, (▲) 316 and (▼) 475 mg l^{-1} of atenolol at pH 3.0 treated at 50–12 mA. The mineralization current efficiency for the corresponding processes is presented in the inset panels.

158 mg l^{-1} of atenolol because of the production of more quantity of BDD(•OH) from reaction (4) and •OH from Fenton's reaction (2) due to the faster generation of H_2O_2 via reaction (1) [2,3]. At 360 min 94–96% decontamination is always attained, indicating that PEF is very potent even with low currents in the combined cell. However, the inset of Fig. 4a shows that better efficiencies are found at 50–12 mA than at 25–12 mA, at least up to 90 min. This is feasible because when current increases, the process becomes less efficient at long electrolysis times, but the maximum MCE value is achieved at smaller time. While the latter phenomenon can be related to a quicker mineralization of easily oxidizable by-products, the loss in MCE with raising current can be explained by the acceleration of side reactions of hydroxyl radicals giving a relatively lower quantity of organic oxidation events. These waste reactions involve, for example, the oxidation of BDD(•OH) to O_2 by reaction (10) and the dimerization of •OH to H_2O_2 by reaction (11) or its destruction with H_2O_2 by reaction (12). In addition, the relative amount of generated BDD(•OH) can also be reduced by the formation of weaker oxidants

Table 1
Pseudo first-order rate constant and square linear regression coefficient determined for the decay of 158 mg l^{-1} of atenolol in the presence of 0.5 mM Fe^{2+} by EF and PEF processes using single and combined cells at 35 °C, along with the percentage of TOC removed and of nitrogen released after 360 min of electrolysis.

Cell	Current/mA	$k_1 \times 10^3$/s^{-1}	R^2	% TOC removed	% Nitrogen released		
					As NH_4^+	As NO_3^-	Total
EF process							
Pt/ADE	50	0.50	0.992	46	34	3	37
BDD/ADE	50	0.39	0.992	77	58	13	71
Pt/ADE–Pt/CF	50–12	2.03	0.983	81	59	6	65
BDD/ADE–Pt/CF	50–12	1.56	0.982	90	73	12	85
PEF process							
Pt/ADE	50	0.75	0.990	83	65	12	77
BDD/ADE	50	0.74	0.985	95	68	19	87
Pt/ADE–Pt/CF	50–12	1.95	0.986	95	72	10	82
BDD/ADE–Pt/CF	50–12	2.03	0.986	97	67	19	86

such as $S_2O_8^{2-}$ by reaction (13) and ozone by reaction (14) [2]:

$$2BDD(^{\bullet}OH) \rightarrow 2BDD + O_{2(g)} + 2H^+ + 2e^- \quad (10)$$

$$2^{\bullet}OH \rightarrow H_2O_2 \quad (11)$$

$$H_2O_2 + {}^{\bullet}OH \rightarrow HO_2^{\bullet} + H_2O \quad (12)$$

$$2SO_4^{2-} \rightarrow S_2O_8^{2-} + 2e^- \quad (13)$$

$$3H_2O \rightarrow O_{3(g)} + 6H^+ + 6e^- \quad (14)$$

The effect of pH on the TOC decay of 158 mg l^{-1} atenolol is depicted in Fig. 4b. For the experiments at pH 4.0 and 6.0, the solution pH was continuously regulated at its initial value by adding small volumes of 1 M NaOH because of its rapid acidification due to the production of acidic by-products. As can be observed, the fastest degradation with higher mineralization degree takes place at pH 3.0, very close to the optimum pH of 2.8 for Fenton's reaction (2) [22]. That means that in PEF this reaction limits the mineralization process of organics, although the high efficiency of this procedure can be accounted for by the rapid destruction of final intermediates by BDD(•OH) and/or their photodecomposition by UVA light.

The efficient mineralization for increasing atenolol concentrations by PEF in a BDD/ADE-Pt/CF cell operating at optimized conditions of pH 3.0 and currents of 50–12 mA is depicted in Fig. 4c. This method is so potent that 95% TOC removal is even reached for the higher initial concentration of 475 mg l^{-1} in 360 min. The MCE values for this process then increase with increasing drug content, as shown in the inset of Fig. 4c. For example, maximum efficiencies close to 100% are obtained at 120 min for 316 mg l^{-1} and at 180–240 min for 475 mg l^{-1}. This behavior suggests the existence of a gradual inhibition of waste reactions of hydroxyl radicals like reactions (11) and (12) with raising the organic matter and hence, more amounts of these radicals are able to destroy higher quantities of pollutants promoting their quicker mineralization and increasing efficiency.

3.4. Decay kinetics for atenolol

The synergistic action of the different generated oxidants (•OH, BDD(•OH) and/or Pt(•OH)) and UVA light was analyzed by measuring the atenolol concentration decay for the trials of Fig. 3a by reversed-phase HPLC. The *C*-time plots thus obtained are shown in Fig. 5a, whereas the corresponding kinetic analysis assuming a pseudo first-order reaction for the drug is depicted in Fig. 5b. From the excellent linear straights found, the pseudo first-order rate constant (k_1) and the square linear regression coefficient (R^2) were determined for each system, being collected in Table 1.

It is well-known that in EF, •OH produced from Fenton's reaction (2) reacts much more rapidly with aromatic pollutants than BDD(•OH) or Pt(•OH) [18,19,21]. Although the fall of atenolol by this method in Pt/ADE and BDD/ADE single cells can be related to its quick reaction with •OH, Fig. 5a evidences its faster removal under the former conditions. This suggests a strong adsorption of this compound at the Pt anode surface favoring its attack by Pt(•OH), while it is more slowly destroyed with BDD(•OH) on BDD where it is expected to be weakly adsorbed [2]. When the combined Pt/ADE–Pt/CF and BDD/ADE–Pt/CF cells are used in EF, the atenolol decay is strongly accelerated with k_1-values about four times higher than those of the single cells (see Table 1). This corroborates the efficient Fe^{2+} regeneration at the CF cathode, enhancing •OH production from Fenton's reaction (2) in both combined cells. Compared with EF, a slight enhancement of the rate of drug removal can be observed in Fig. 5a by applying PEF in both singles cells,

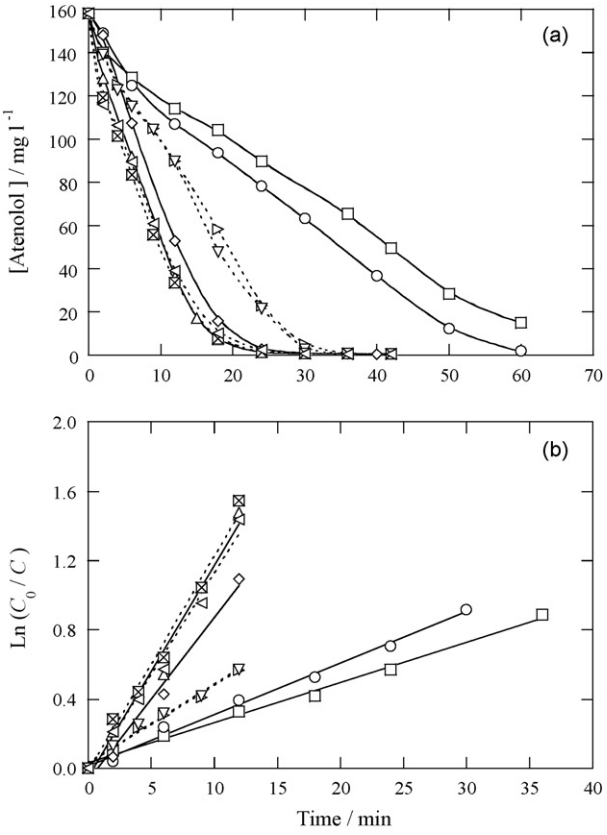

Fig. 5. (a) Atenolol concentration decay with time for the same solution as Fig. 3. Method: (○) EF in Pt/ADE cell at 50 mA, (□) EF in BDD/ADE cell at 50 mA, (△) EF in combined Pt/ADE–Pt/CF cell at 50–12 mA, (◊) EF in combined BDD/ADE–Pt/CF cell at 50–12 mA, (▽) PEF in Pt/ADE cell at 50 mA, (▷) PEF in BDD/ADE cell at 50 mA, (◁) PEF in combined Pt/ADE–Pt/CF cell at 50–12 mA and (⊠) PEF in combined BDD/ADE–Pt/CF cell at 50–12 mA. (b) Kinetic analysis assuming a pseudo first-order reaction of atenolol with electrogenerated hydroxyl radicals.

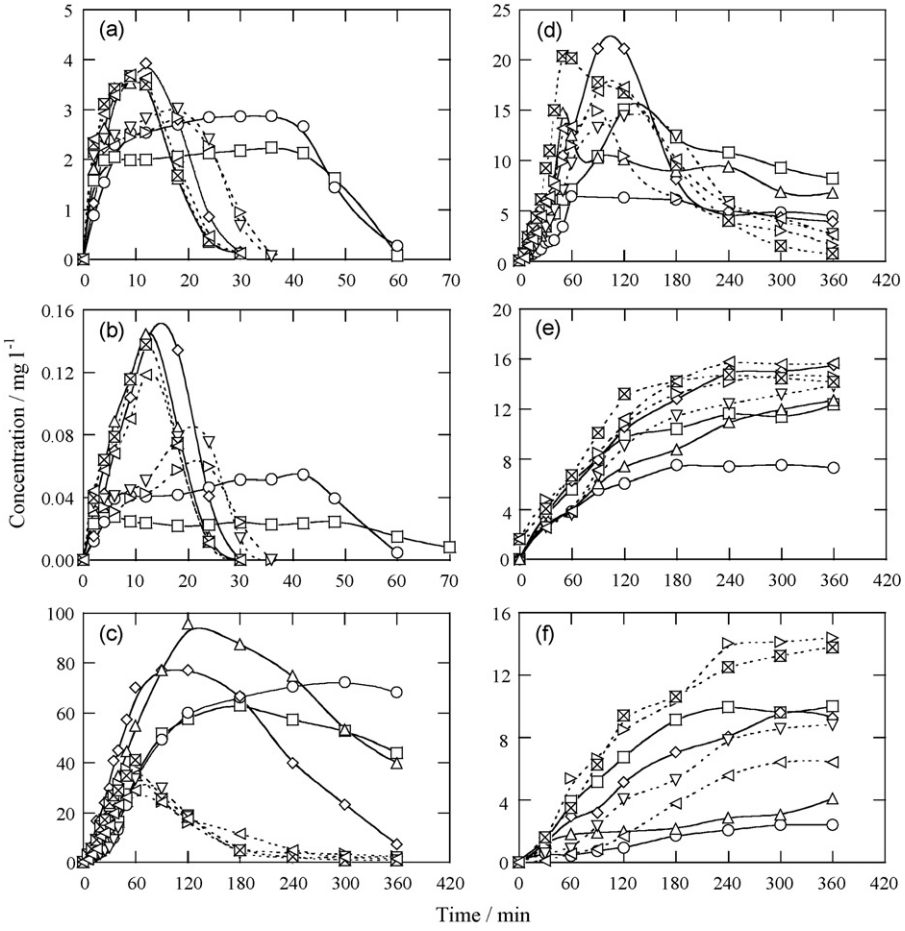

Fig. 6. Evolution of the concentration of selected by-products formed during the degradation of 158 mg l^{-1} of atelonol under the same conditions as in Fig. 5. (a) 4-Hydroxyphenylacetamide, (b) *p*-benzoquinone, (c) oxalic acid, (d) oxamic acid, (e) NH_4^+ ion and (f) NO_3^- ion.

increasing the corresponding k_1-value in ca. 1.5 times (see Table 1). This can be related to the extra production of •OH via the photolytic reaction (5), since blank experiments showed that atenolol is not directly photodecomposed by UVA irradiation. Fig. 5a also shows that the use of PEF in both combined cells yields again a much more rapid destruction of this compound, indicating that greater amounts of oxidant •OH are formed from Fe^{2+} regeneration at the CF cathode than under the action of UVA light. As an evidence of the preponderance of the former process, note that a similar k_1-value of 2×10^{-3} s^{-1} is found for the combined cells under both EF and PEF conditions (see Table 1).

Previous work on the EF and PEF treatments of other aromatic pharmaceuticals with single Pt/O_2 and BDD/O_2 cells [14,15,18,19,21] showed that increasing applied current or decreasing initial pollutant concentration causes greater k_1-values, i.e., an enhancement of their destruction rate, along with a shorter electrolysis time and lower energy cost for reaching >95% TOC removal, as also observed in Fig. 4a and c, respectively, for the PEF process of atenolol in a BDD/ADE-Pt/CF cell. This indicates that the EF and PEF methods with the proposed combined cells, which yield faster decontamination rates than single cells (see Table 1), are feasible to be applied to real effluents with few micrograms per liter of atenolol allowing their fast overall removal with very low cost.

3.5. Time-course of intermediates

GC–MS analysis of short-time electrolyzed solutions in the less oxidant Pt/ADE cell revealed the formation of acetamide [m/e = 59 (100, M^+)] at retention time (t_r) of 4.24 min and *p*-benzoquinone [m/e = 108 (100, M^+)] at t_r = 6.71 min. After ethylation, only the diethylated derivative of oxalic acid [m/e = 146 (2, M^+)] at t_r = 8.12 min was detected. Nevertheless, 4-hydroxyphenylacetamide, expected as precursor of acetamide and *p*-benzoquinone, was only detected by reversed-phase HPLC. These chromatograms exhibited peaks associated with 4-hydroxyphenylacetamide at t_r = 3.8 min and its derivative *p*-benzoquinone at t_r = 5.1 min. Both aromatics were unequivocally identified by comparing their retention times and UV–Vis spectra, measured on the photodiode array detector, with those of pure standards. The evolution of these intermediates in the systems tested is presented in Fig. 6a and b, respectively. As can be seen, both species persist in the medium while the initial drug is being oxidized (see Fig. 5a), although they are accumulated in very low content in all cases. This is indicative of a quick destruction of aromatic contaminants by •OH.

A different behavior was detected for generated carboxylic acids. Ion-exclusion chromatograms of electrolyzed solutions displayed well-defined peaks related to oxalic (t_r = 6.4 min), tartronic (t_r = 7.6 min), maleic (t_r = 8.0 min), tartaric (t_r = 8.4 min), oxamic (t_r = 9.1 min), glycolic (t_r = 12.0 min), formic (t_r = 13.6 min) and fumaric (t_r = 15.1 min) acids. In all treatments, these acids or better their iron complexes disappeared in less of 240 min, except oxalic and oxamic that persisted up to the end of electrolysis, as shown in Fig. 6c and d, respectively. Both figures evidence that Fe(III)-oxalate and Fe(III)-oxamate complexes attain a steady concentration in EF using a Pt/ADE cell, indicating that they are not oxidized by Pt(•OH) and •OH. However, both complexes are slowly destroyed by BDD(•OH) using a BDD/ADE cell, as expected from the greater oxi-

dation ability of BDD on carboxylic acids [2]. This behavior varies for EF in the combined Pt/ADE–Pt/CF and BDD/ADE–Pt/CF cells, where higher amounts of both acids are formed and destroyed, much more quickly for the latter configuration. Since Fe^{2+} is largely regenerated at the CF cathode of both combined cells, one can assume [5,7] that Fe(II)-oxalate and Fe(II)-oxamate complexes are competitively formed and oxidized with •OH in both cases, as well as with BDD(•OH) in the BDD/ADE–Pt/CF cell, thus strongly enhancing their mineralization processes in relation to those of single cells (see Fig. 3a). In contrast, the photolysis of Fe(III) and Fe(II) complexes

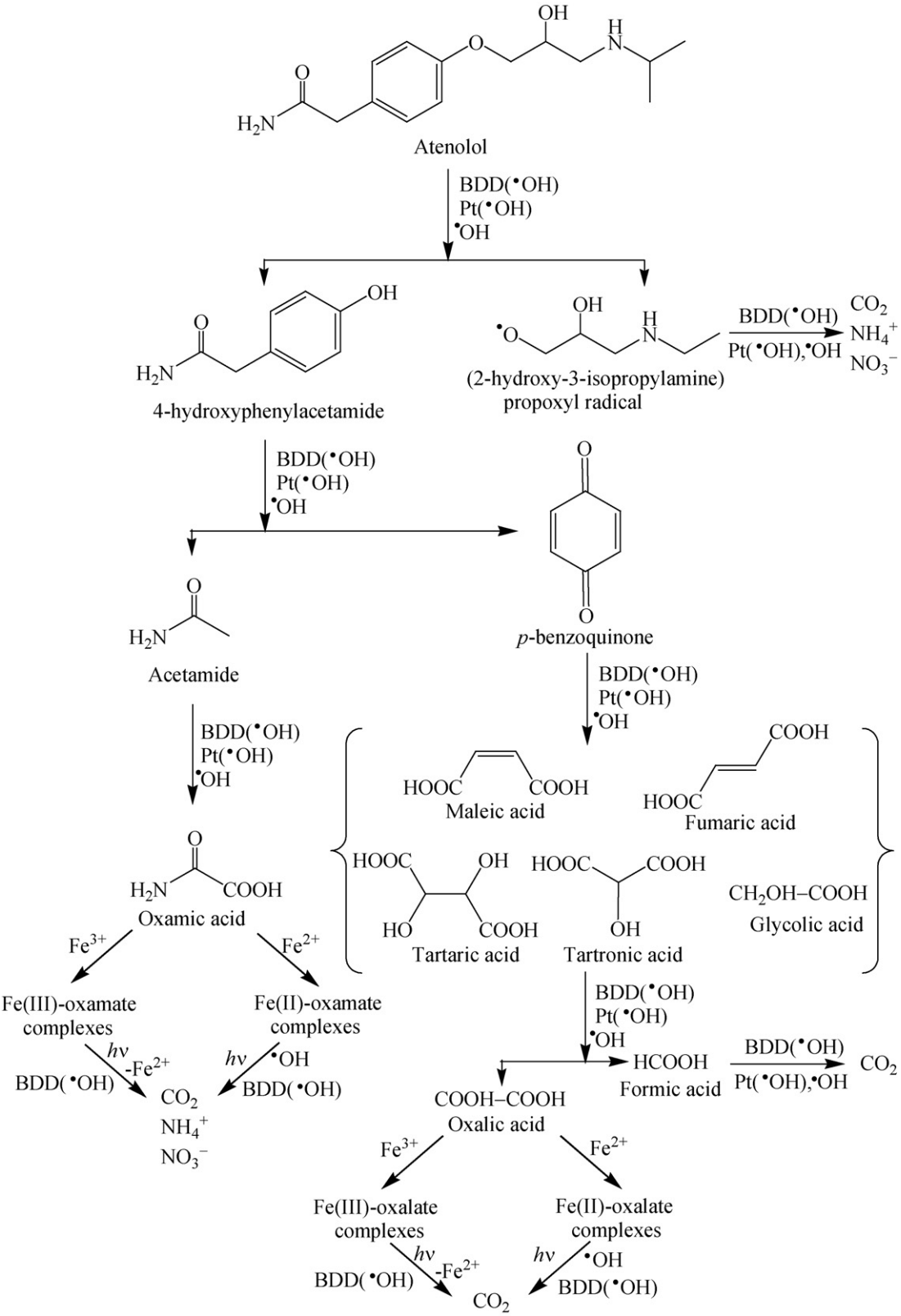

Fig. 7. Proposed reaction sequence for atenolol mineralization by EF and PEF. Oxidant hydroxyl radicals are denoted like BDD(•OH) and Pt(•OH) when they are electrogenerated at the BDD and Pt anode surface, respectively, and like •OH when it is produced in the medium.

of both acids accounts for by their quick decay at similar rate using PEF in all single and combined systems (see Fig. 6c and d), yielding almost total mineralization at the end of all these treatments.

Ionic chromatography showed that ammonium and nitrate ions were produced during the mineralization process of atenolol. However, other possible nitrogen by-products such as nitrite ions were not detected. Fig. 6e and f evidence that both ions are progressively released to the medium, with a larger formation of NH_4^+ in all EF and PEF processes. This fact can also be deduced from the much higher percentage of N released as NH_4^+ than as NO_3^- calculated after 360 min of all electrolyses and collected in Table 1. These data are indicative of an enhancement of NO_3^- generation using a BDD anode, suggesting that the oxidation of *N*-intermediates with BDD(•OH) promotes the formation of this anion. Results of Table 1 also show that only 87% of initial N is converted into inorganic ions when 95–97% mineralization is achieved in PEF, suggesting that part of initial N is loss as volatile *N*-products, probably NO_x species.

3.6. Reaction sequence

Fig. 7 presents a proposed general pathway for the mineralization of atenolol by EF and PEF. The main oxidizing agents are the electrogenerated hydroxyl radicals BDD(•OH), Pt(•OH) and •OH, although parallel slower degradation with other weaker oxidants (H_2O_2, $S_2O_8^{2-}$, O_3, etc.) is also feasible. Fe(II) and Fe(III) complexes of carboxylic acids are only given for oxalic and oxamic for sake of simplicity. The initial breaking of the lateral chain of atenolol via C(4)–O bond gives 4-hydroxyphenylacetamide and (2-hydroxy-3-isopropylamine)propoxyl radical, which is oxidized to CO_2, NH_4^+ and NO_3^-. Hydroxylation on C(1)-position of 4-hydroxyphenylacetamide, followed by dehydrogenation of –OH groups, leads to *p*-benzoquinone with loss of acetamide that is subsequently transformed into oxamic acid [14]. Further degradation of *p*-benzoquinone yields a mixture of maleic, fumaric, tartaric, tartronic and glycolic acids. These compounds are then oxidized to oxalic and formic acids as ultimate by-products [14,15,18,19,21]. Formic acid is converted into CO_2 in all treatments, but the destruction of oxalic and oxamic acids depends on the system tested. Both acids form Fe(III) complexes in single cells and also Fe(II) complexes in combined cells thanks to the fast Fe^{2+} regeneration at the CF cathode. While both kinds of complexes are slowly degraded by BDD(•OH) in EF and much more rapidly photodecomposed under UVA irradiation in PEF, Fe(II)-oxalate and Fe(II)-oxamate complexes are also destroyed by •OH. NH_4^+ and NO_3^- ions are produced during the degradation of Fe(III)-oxamate and Fe(II)-oxamate species [14].

4. Conclusions

It has been demonstrated that the use of four-electrode combined cells with an ADE cathode for H_2O_2 electrogeneration and a CF cathode for Fe^{2+} regeneration accelerates the degradation and the decay of the drug β-blocker atenolol by EF and PEF compared with two-electrode cells. The former cells enhance the •OH production from Fenton's reaction (2) that promotes the destruction of aromatic pollutants. Since BDD(•OH) has much greater oxidation ability than Pt(•OH), the BDD/ADE–Pt/CF cell has higher oxidation power and is more efficient than the Pt/ADE–Pt/CF one for the EF treatment. However, for the PEF process, the synergistic action of UVA light promoting in lower proportion the generation of more amounts of •OH from photolytic reaction (5), but rapidly photolyzing iron complexes of generated carboxylic acids, causes the almost overall mineralization of the drug in all single and combined cells. The highest degradation rate is reached for the BDD/ADE–Pt/CF system, which operates at optimum conditions at pH 3.0 and its efficiency rises with decreasing current and increasing drug concentration. The decay of atenolol always follows a pseudo first-order reaction. 4-Hydroxylphenylacetamide and *p*-benzoquinone detected at low contents as aromatic intermediates persist in the medium while the drug is being oxidized. Oxalic and oxamic acids are the most persistent carboxylic acids. Their Fe(III) complexes formed in the single cells can only be destroyed by BDD(•OH) or photolyzed by UVA light, whereas their competitive Fe(II) complexes also produced in the combined cells are oxidized with •OH, thus explaining the highest oxidation power of such kind of configurations. The initial N of atenolol is released as NH_4^+ and in smaller proportion as NO_3^-, although the latter anion is comparatively produced in larger extent using the BDD anode.

Acknowledgements

The authors are grateful to MEC (Ministerio de Educación y Ciencia, Spain) for financial support under project CTQ 2007-60708/BQU, cofinanced with Feder funds, and to CONACYT (Consejo Nacional de Ciencia y Tecnología, Mexico) for the grant given to E. Isarain-Chávez.

References

[1] S. Parsons (Ed.), Advanced Oxidation Processes for Water and Wastewater Treatment, IWA Publishing, London, 2004.
[2] M. Panizza, G. Cerisola, Chem. Rev. 109 (2009) 6541–6569.
[3] E. Brillas, I. Sirés, M.A. Oturan, Chem. Rev. 109 (2009) 6570–6631.
[4] M. Diagne, N. Oturan, M.A. Oturan, Chemosphere 66 (2007) 841–848.
[5] I. Sirés, J.A. Garrido, R.M. Rodríguez, E. Brillas, N. Oturan, M.A. Oturan, Appl. Catal. B: Environ. 72 (2007) 382–394.
[6] I. Sirés, N. Oturan, M.A. Oturan, R.M. Rodríguez, J.A. Garrido, E. Brillas, Electrochim. Acta 52 (2007) 5493–5503.
[7] M.A. Oturan, M. Pimentel, N. Oturan, I. Sirés, Electrochim. Acta 54 (2008) 173–182.
[8] A. Özcan, Y. Şahin, K. Savaş, M.A. Oturan, J. Hazard. Mater. 153 (2008) 718–727.
[9] S. Hammami, N. Bellakhal, N. Oturan, M.A. Oturan, M. Dachraoui, Chemosphere 73 (2008) 678–684.
[10] B. Balci, N. Oturan, R. Cherrier, M.A. Oturan, Water Res. 43 (2009) 1924–1934.
[11] E. Brillas, J.C. Calpe, J. Casado, Water Res. 34 (2000) 2253–2262.
[12] E. Brillas, M.A. Baños, J.A. Garrido, Electrochim. Acta 48 (2003) 1697–1705.
[13] A. Da Pozzo, L. Di Palma, C. Merli, E. Petrucci, J. Appl. Electrochem. 35 (2005) 413–419.
[14] I. Sirés, J.A. Garrido, R.M. Rodríguez, P.L. Cabot, F. Centellas, C. Arias, E. Brillas, J. Electrochem. Soc. 153 (2006) D1–D9.
[15] I. Sirés, C. Arias, P.L. Cabot, F. Centellas, J.A. Garrido, R.M. Rodríguez, E. Brillas, Chemosphere 66 (2007) 1660–1669.
[16] G.R. Agladze, G.S. Tsurtsumia, B.-I. Jung, J.-S. Kim, G. Gorelishvili, J. Appl. Electrochem. 37 (2007) 985–990.
[17] H. Wang, J. Wang, Appl. Catal. B: Environ. 77 (2007) 58–65.
[18] M. Skoumal, C. Arias, P.L. Cabot, F. Centellas, J.A. Garrido, R.M. Rodríguez, E. Brillas, Chemosphere 71 (2008) 1718–1729.
[19] E. Guinea, C. Arias, P.L. Cabot, J.A. Garrido, R.M. Rodríguez, F. Centellas, E. Brillas, Water Res. 42 (2008) 499–511.
[20] M. Panizza, G. Cerisola, Water Res. 43 (2009) 339–344.
[21] M. Skoumal, R.M. Rodríguez, P.L. Cabot, F. Centellas, J.A. Garrido, C. Arias, E. Brillas, Electrochim. Acta 54 (2009) 2077–2085.
[22] Y. Sun, J.J. Pignatello, Environ. Sci. Technol. 27 (1993) 304–310.
[23] R.G. Zepp, B.C. Faust, J. Hoigné, Environ. Sci. Technol. 26 (1992) 313–319.
[24] Y. Zuo, J. Hoigné, Environ. Sci. Technol. 26 (1992) 1014–1022.
[25] M. Cleuvers, Chemosphere 59 (2005) 199–205.
[26] E. Zuccatto, S. Castiglioni, R. Fanelli, J. Hazard. Mater. 122 (2005) 205–209.
[27] L.N. Nikolai, E.L. McClure, S.L. MacLeod, C.S. Wong, J. Chromatogr. A 1131 (2006) 103–109.
[28] K. Fent, A.A. Weston, D. Caminada, Aquat. Toxicol. 76 (2006) 122–159.
[29] N. Vieno, T. Tuhkanen, L. Kronberg, Water Res. 41 (2007) 1001–1012.
[30] M. Maurer, B.I. Escher, P. Richle, C. Schaffner, A.C. Alder, Water Res. 41 (2007) 1614–1622.
[31] J. Winter, A.D. Lillicrap, J.E. Caunter, C. Schaffner, A.C. Alder, M. Ramil, T.A. Ternes, E. Giltrow, J.P. Sumpter, T.H. Hutchinson, Aquat. Toxicol. 86 (2008) 361–369.
[32] R.N. Hegde, N.P. Shetti, S.T. Nandibewoor, Polyhedron 28 (2009) 3499–3506.
[33] E. Marco-Urrea, J. Radjenović, G. Caminal, M. Petrović, T. Vicent, D. Barceló, Water Res. 44 (2010) 521–532.
[34] F.J. Welcher (Ed.), Standard Methods of Chemical Analysis, Vol. 2, Part B, 6th ed., R.E. Krieger Publishers Co., Huntington, New York, 1975, p. 1827.
[35] N.H. Furman (Ed.), Standard Methods of Chemical Analysis, vol. 1, 6th ed., R.E. Krieger Publishers Co., Huntington, New York, 1975, p. 553.
[36] E.B. Sandell, in: B.L. Clarke, P.J. Elving, I.M. Kolthoff (Eds.), Chemical Analysis, vol. III, 3rd ed., Interscience Publishers, Inc., New York, 1959, p. 522.